**Sudan University of Science and Technology**

**College Graduate Studies**

# Investigation of Structure and Magnetic Properties of Cobalt Ferrite Nanoparticles Prepared by Combustion, Hydrothermal and Glycol thermal Methods.

# التحقق من التركيب والخصائص المغناطيسية لمركب الكوبالت فرايت النانوي المحضر بطريقة الإحتراق والطريقة الحرارية المائية وطريقة الجلايكول الحرارية.

**A Dissertation Submitted in Partial Fulfilment for the Requirement of a Master Degree (M. Sc) in Physics**

**Prepared by**

**Sara Khalid Khidir Mohamed**

**Supervised by**

**Dr. Nadir S.E. Osman**

July -2018

# الآيـة

قال تعالي :

"يَرْفَعِ اللَّهُ الَّذِينَ آمَنُوا مِنكُمْ وَالَّذِينَ أُوتُوا الْعِلْمَ دَرَجَاتٍ وَاللَّهُ بِمَا تَعْمَلُونَ خَبِيرٌ"

سورة المجادلة الآية رقم 11

# Dedication

*I dedicate this work to my parents and*
*To my colleagues in the Faculty of Science, Sudan University of Science and Technology, and all my friends my fiancé, to those who helped me and supported me in this* work.

# Acknowledgments

First, I pay innumerable gratitude to Allah who gave me the strength, courage and knowledge to complete this research successfully.

I would like to thank my supervisor Dr. Nadir S.E Osman for being the source of inspiration, patience, and motivation. I had been extremely lucky to have a supervisor who cared so much about my work, and who responded to my questions and queries so promptly.

I wish to express my appreciation to all the individuals who help me to write this research. Special thanks to all staff members at physic Department, Faculty of Science, Sudan University of Science and Technology.
Great acknowledge goes to University of KwaZulu-Natal, Westville campus for synthesis and characterization facilities used in this work.

Finally, I must express my very profound gratitude to my family and friends for providing me with unfailing support and continuous encouragement throughout my years of study and through the process of researching and writing this thesis, this accomplishment would not have been possible without them thank.

# Abstract

In this work cobalt ferrite ($CoFe_2O_4$) nanoparticles were produced by combustion, hydrothermal and glycol thermal methods. The aim is to study the effect of the synthesis methods upon structure and magnetic properties of the obtained nanoparticles. The structure was studied by X-rays diffraction (XRD) and high resolution transmission electron microscope (HRTEM). XRD results confirm the formation of cubic spinel structure with crystallite sizes of 23.296 nm, 7.910 nm and 9.168 nm for combustion, hydrothermal and glycol thermal methods, respectively. The X-rays patterns of the studies samples were fitted using Full Proof software program. The obtained lattice parameters were 8.339Å, 8.352 Å and 8.383 Å for combustion, hydrothermal and glycol thermal methods respectively. The lattice parameters were also calculated using Bragg's law from the highest intensity peak (311) and found to be 8.3716 Å, 8.3455 Å and 8.3657 Å for combustion, hydrothermal and glycol thermal methods, respectively. The sample prepared by combustion method showed the lowest value of microstrain of 0.00501±0.00010. Significant correlation was observed between microstrains and lattice parameters. The obtained images from high resolution transmission electronic microcopy (HRTEM) confirmed the XRD results and reflected well crystalline structure of the synthesized $CoFe_2O_4$ nanoparticles. The magnetic properties were studied by vibrating sample magnetometer (VSM). The results showed that the highest value of maximum magnetization of 56.06 emu/g was for the sample prepared by combustion method. Whilst, the obtained maximum magnetizations of 47.74 emu/g and 32.71 emu/g were for the samples prepared by hydrothermal and glycol thermal methods, respectively. The obtained value of corecivity were 1277.6 Oe, 175.12 Oe and 199.95 Oe for the sample prepared by combustion, hydrothermal and glycol thermal methods, respectively. It can be concluded that various synthesis methods of nanoparticle can lead to different structural properties and then significantly affect the magnetic properties. In particular, maximum magnetization and corecivity increases as crystallite sizes increases.

# المستخلص

في هذا البحث تم إنتاج جزيئات مركب الكوبالت- فرايت النانوية بطريقة الإحتراق والطريقة الحرارية المائية وطريقة الجلايكول الحرارية والهدف من ذلك دراسة تأثيرطريقة التصنيع علي التركيب والخواص الفيزيائية للجزئيات النانوية. عند دراسة التركيب البلوري عن طريق جهاز انحراف الأشعة السينية والمجهر الالكتروني النافذ عالي الدقة أكدت النتائج تكوين الماده بحجم بلوري يعادل 23.296 و710 و 9.168 نانومتر بطريقة الإحتراق والطريقة الحرارية المائية وطريقة الجلايكول الحرارية على التوالي، ومن الأنماط الناتجة عن دراسة العينات المختلفة في جهاز إنحراف الأشعة السينية تم حساب معامل الشبيكة ووجد أنه يساوي 8.339 و 8.352 و8.383 أنجستروم بطريقة الاحتراق والطريقة الحرارية المائية وطريقة الجلايكول الحرارية على التوالي وأيضا تم حساب معامل الشبيكة لأعلى قمة موجودة (311) ووجد أنه يساوي 8.3716 و 8.3455 و 8.3657 أنجستروم بطريقة الإحتراق والطريقة الحرارية المائية وطريقة الجلايكول الحرارية على التوالي. أصغر قيمة للإجهاد وجدت في العينة المحضرة بطريقة الإحتراق وتساوي 0.00501. لوحظ إرتباط بين الإجهاد وثابت الشبيكة. الصورة الناتجة من جهاز إنحراف الأشعة السينية تلائم تلك الناتجة عن المجهر الإلكتروني النافذ عالي الدقة وتعكس جيدا التركيب والشكل البلوري لجزيئات الكوبالت- فرايت النانوية.

تم دراسة الخواص المغناطيسية بواسطة جهاز مقياس المغنطيسية والنتائج توضح أن القيمة العليا للمغنطيسية سجلت للعينة التي تم تحضيرها بواسطة طريقة الإحتراق كانت تساوي 56.06 emu/g. بينما القيمة العليا للمغنطيسية في العينات التي تم تحضيرها بواسطة الطريقة الحرارية المائية والجلايكول الحراري تساوي 47.74 و 32.7106 emu/g على التوالي. ووجد أن الممانعة المغنطيسية تعادل 1277.6 و175.12 و 199.5 الاورستد بطريقة الإحتراق والطريقة الحرارية المائية وطريقة الجلايكول الحرارية على التوالي. وأخيرا تؤكد هذه النتائج أن الطرق المختلفة في تركيب المادة النانوية تؤثر على خصائص التركيب وتؤدي إلى تأثير كبير في الخواص المغناطيسية.تحديدا وجد أن القيمة العليا للمغنطيسية و الممانعة المغنطيسية تذيد بذيادة الحجم البلوري للعينات.

# Keywords and acronyms

## Keywords

Nanoparticles, cobalt ferrite, hydrothermal, glycol thermal, combustion, magnetic properties.

## Acronyms

Cobalt ferrite ($CoFe_2O_4$)

X-rays diffraction (XRD)

High resolution transmission electronic microscope (HRTM)

Vibration sample magnetometer (VSM)

# Table of Contents

## ChapterThree

## Experimental details



## Chapter Four

## Results and discussion

# List of Figures

# List of Tables

# Chapter One

# Introduction

# Chapter one

# Theoretical background

## 1.1 Overview

Nano is the measurement unit equal $10^{-9}$ m. The prefix nano is derived from Greek word nannos means dwarf. Theoretical concept of nanoscience was first described in 1959 by Richard Feynman. Nanomaterials have attracted a great attention because of their remarkable physical and chemical properties compared to bulk materials (Horikoshi and Serpone, 2013).

Magnetic nanoparticles with both types soft and hard are widely used in industrial, medical and environmental domains (Lu, 2007). A soft magnetic material which can easily be magnetized and demagnetized has significant features such as high saturation magnetization and permeability, low energy loss as well as low coercive field. These properties make soft magnetic materials to be used in different applications such as in microwave devices, magnetic amplifiers and high frequency devices (Mathew and Juang, 2007). A hard magnetic material cannot be easily demagnetized. These types of materials possesses low permeability and susceptibility, high coercive field and high-energy product (Mathew and Juang, 2007).

Among magnetic materials, ferrites which are ceramic compounds composed of iron oxide $Fe_2O_3$ with metals has many technological applications such as magneto-optic recording medium, high density data storage devises, microwave and electronic devises, electronic inductors, transformers and electromagnets (Khandekar et al., 2011).There are three different types of ferrites namely spinel, garnet and magnetoplumbite (Mathew and Juang, 2007).

Spinel nanoferrites can be considered as the most studied materials because of their interesting optical, magnetic and electrical properties (Nadir S.E. Osman, Thomas Moyo, 2015). Spinel structure has the chemical formula $AB_2O_4$. In normal spinal, A denotes divalent cations occupying tetrahedral sites and B denotes trivalent cations occupying in octahedral sites (Mathew and Juang, 2007).Whenever, the A-sites are completely occupied by trivalent elements and B-sites are occupied by divalent and trivalent elements a ferrite is called inverse spinel (Mathew and Juang, 2007). Changing the divalent elements at the tetrahedral and octahedral sites, magnetic properties of ferrite materials can be tuned (Nadir S.E. Osman and Thomas Moyo, 2015). Figure 1.1 shows the tetrahedral and octahedral sites at spinel structure.

Cobalt ferrite, with a partially inverse spinel structure, is one of the most important of magnetic materials used in different applications such as magnetic recording, ferrofluids technology, biomedical drug delivery and magnetic resonance imaging recording, this is because $CoFe_2O_4$ possesses moderate saturation magnetization, high coercivity, high-density magneto-optic, high chemical stability and electrical insulation (Franco et al., 2007).

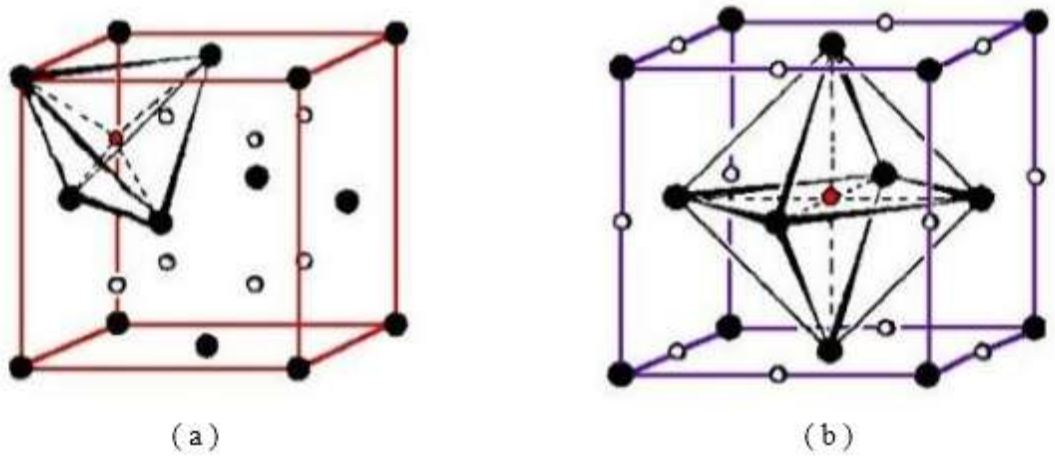


**Figure 1.1.** Tetrahedral (a) and octahedral (b) sites at spinel structure (Sawatzky et al, 1968).

## 1.2 Synthesis mechanisms of nanoparticles

Nanomaterials can be produced using two different mechanisms namely top-down or bottom-up. The approach of top-down involves a process of breaking down bulk sample to create nanostructures. This can be achieved by several techniques such as crushing, milling, pulsed electrochemical etching and vapor deposition. Whilst, bottom-up approach involves chemical methods such as, micro-emulsion, mechano-chemical, sol-gel, co-precipitation, hydrothermal, glycol thermal and combustion methods. These synthesis mechanism of nanomaterials associated with interaction between atoms or molecules to form nano structure (Peng et al., 2011).

## 1.3 Types of magnetic materials

Magnetic materials can be classified based on their response to an externally applied magnetic field into five main types namely ferromagnetic, paramagnetic, diamagnetic, ferrimagnetic and antiferromagnetic as shown in Figure 1.2.

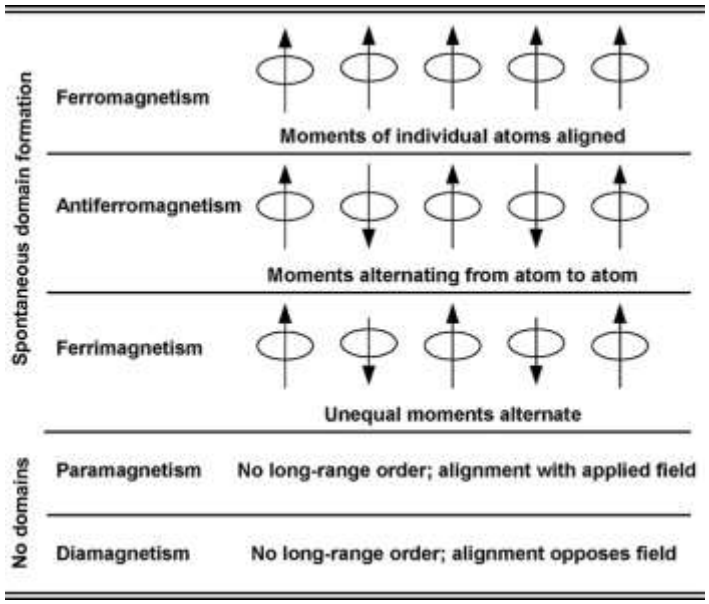


**Figure 1.2.** Types of magnetic materials (Mathew and Juang, 2007).

### 1.3.1 Ferromagnetic

A ferromagnetic material such as iron, nickel, and cobalt has net magnetic moments due to unpaired electrons. This type of materials has domains each one contains large number of atoms with magnetic moments pointing to the same direction. However, the domains are randomly distributed giving permanent net magnetic moments to the material. (Jr., 1940).

### 1.3.2 Antiferromagnetic

Antiferromagnetic materials such as MnO, CoO, NiO, and $CuCl_2$ are compounds of two different atoms that occupy different lattice sites. The two atoms have magnetic moments that are equal in magnitude and opposite in direction which results in zero net magnetic moments. If the coupling of electron spins are in antiparallel alignment, then spins will cancel, each other and no net magnetic moments arise (Nagamiya, 1951).

### 1.3.3 Ferrimagnetic

Ferrimagnetic materials such as magnetite $Fe_3O_4$ residing on different lattice sites with antiparallel magnetic moments. However, in these type of materials, the magnetic moments do

not cancel out because they have different magnitudes which lead to net spontaneous magnetic moments (Dekker, 1981).

### 1.3.4 Paramagnetic

Paramagnetic materials have a magnetic moments that align along the direction of the applied magnetic field forming a weak net magnetic moment. These materials do not retain magnetic moment when the magnetic field is remove (Krasnovyd et al., 2015).

### 1.3.5 Diamagnetic

Diamagnetic materials such as Cu, Ag, and Au have no unpaired electrons which results in zero net magnetic moments. These materials have a very weak response against the applied magnetic field. Realignment of the electron orbits is possible when the applied magnetic field is very strong. They do not retains magnetic moment when the magnetic field is removed (Simon and Geim, 2000).

## 1.4 Literature review

Since magnetic properties of cobalt ferrite ($CoFe_2O_4$) nanoparticles are highly affected by sizes and shapes, many efforts have been need to produce a fine and monodisperse $CoFe_2O_4$ nanoparticles. Literature survey reveals that many methods have been used in preparing cobalt ferrite ($CoFe_2O_4$) nanoparticles.

Adolfo Franco Ju´ nior et al (2007) synthesized of by $Co_x\ Fe_{(3-x)}\ O_4$ by combustion reaction method. Structural and magnetic properties of the products were investigated by X-rays diffraction, scanning electron microscopy, Fourier transform infrared spectroscopy and vibrating sample magnetometer. The crystallite size was found for $x$=0 equal 26.86 nm. The magnetic properties measured at room temperature such as saturation magnetization, remanence magnetization and coercivity field, were 48 emu/g, 15 emu/g and 900 Oe, respectively (Adolfo Franco, 2007).

Jianhong Peng et al (2011) studied the magnetic properties of gadolinium-doped cobalt ferrite $CoFe_{2-x}Gd_xO_4$ ($x$ = 0 - 0.25) synthesized by hydrothermal methods. From the analyses of X-rays diffraction found that the average crystallite size equal 9.7 nm when $x$=0. The magnetic properties investigated by vibrating sample magnetometer .The coercivity ($H_c$) was found equal 996 Oe for $x$ = 0 (Peng, 2011).

Mahboubeh Houshiar et al (2014) prepared the cobalt ferrite ($CoFe_2O_4$) nanoparticles using combustion, co-precipitation and precipitation methods. Comparison was made for size, structural and magnetic properties. The structure of $CoFe_2O_4$ nanoparticles was studied by X-rays diffraction technique. XRD data analysis showed average size was 69.5 nm for combustion samples. The magnetic properties were calculated by vibrating sample magnetometer. VSM data of samples showed a saturation point in the magnetic field of less than 15 kOe. Magnetization saturation ($M_s$) was 56.7emu/g for combustion synthesized. Coercivity ($H_c$) was 2002 Oe for combustion synthesized samples (Mahboubeh Houshiar, 2014).

Nadir S.E. Osman and Thomas Moyo (2015) synthesized $CoFe_2O_4$ nano ferrite simultaneously substituted by Mg, Sr and Mn by glycol thermal technique. The average crystallite size, lattice parameter, X-rays density and microstrain were calculated from X-rays diffraction data and the average crystallite size confirmed by high-resolution transmission electron microscopy. The magnetic properties were investigated for $Mg_xSr_xMn_xCo_{1-3x}Fe_2O_4$ by vibration sample magnetometer. The crystallite size was found for $x$=0 equal 8.27 nm and the coercivity equal 397.70 Oe (Nadir S.E. Osman and Thomas Moyo, 2015).

Rohollah Safi et al (2016) studied the structure refinement, cations distribution and magnetic features of $CoFe_2O_4$ nanoparticles synthesized by co-precipitation, hydrothermal, and combustion methods. X-rays diffraction analysis (XRD), and vibrating sample magnetometer (VSM) were used to investigate the structural characteristics and magnetic properties of cobalt ferrite nanocrystals. The average crystallite size was 18 and 178 nm for hydrothermal and combustion methods, respectively (Rohollah Safi, 2016).

## 1.5 Research problem

Structural and magnetic properties of cobalt ferrite ($CoFe_2O_4$) nanoparticles are excepted to be affected by synthesis method. This work aims to investigate the effect of hydrothermal, combustion and glycol thermal methods on structural and magnetic properties of $CoFe_2O_4$.

## 1.6 Objectives

- To obtain of $CoFe_2O_4$ nanoparticles by combustion, hydrothermal, glycol thermal methods.
- To identify spinel structural of the synthesized $CoFe_2O_4$ by X-rays diffraction technique.

- To refine the XRD results using Full proof software in order to obtain the structure parameters.
- To investigate the magnetic properties of the synthesized $CoFe_2O_4$ nanoparticles.

## 1.7 Thesis layout

This thesis consists of four chapters. Chapter one, gives general introduction about, spinel structure, synthesis of nanoparticles, types of magnetic materials and literature review, in addition to research problem and objectives. Chapter two describes theoretical background about origin of magnetism. Materials and methods are shown in chapter three. Results, discussion, conclusion, recommendations and future work are presented in chapter four.

# Chapter Two

# Theoretical background

# Chapter two

# Theoretical background

This chapter discus the theoretical background of the origin of the magnetism, magnetization and also contains of description of Bohr theory of magnetism

## 2.1 Origin of magnetism

Magnetism was discovered by Sir Humphrey Davy at 1755 in England (Coey and Coey, 2010). Origin of name from the Greek word Magnesia is a district of Thessaly. Magnetism describes the phenomenon of forces between two or more objects that are related to a magnetic field. Magnetism originates from the spin and orbital magnetic moment of an electron are oppositely directed (Coey and Coey, 2010). The orbital motion of an electron around the nucleus is similarly to an electrical circuit which is given by

$$\mu_e = I\pi r^2 = -\pi r^2 \left(\frac{ev}{2\pi r}\right) = -\frac{e\omega\pi r^2}{2\pi} = -\frac{e\omega r^2}{2}, \qquad 2.1$$

where *I* is the current, e the electronic charge, $\mu_e$is the orbital magnetic moment, $\omega$ is the frequency, *v* velocity and *r* is the radius of electron orbit. The magnitude of the orbital angular momentum $\vec{l}$ of an electron is given by

$$\vec{l} = m_e\, v\, r = \ m_e\, \omega r^2, \qquad 2.2$$

where $m_e$ the mass. From 2.1 and 2.2 the relationship between the orbital magnetic moment $\mu_l$ and the orbital angular momentum $\vec{l}$ of an electron can be written as

$$\mu_l = \frac{-e\,\vec{l}}{2m_e} \qquad 2.3$$

Similarly the magnetic moment due to intrinsic spin angular momentum of an electron $\vec{s}$ is given by

$$\mu_s = \frac{-e\,\vec{s}}{2m_e} \qquad 2.4$$

## 2.2 Bohr theory of magnetism and spin moment

The quantum theory of matter which was discovered by Bohr in 1913, postulates that the electron orbit around the nucleus of the atom originates the magnetic behavior of matter as shows in figure 2.1.

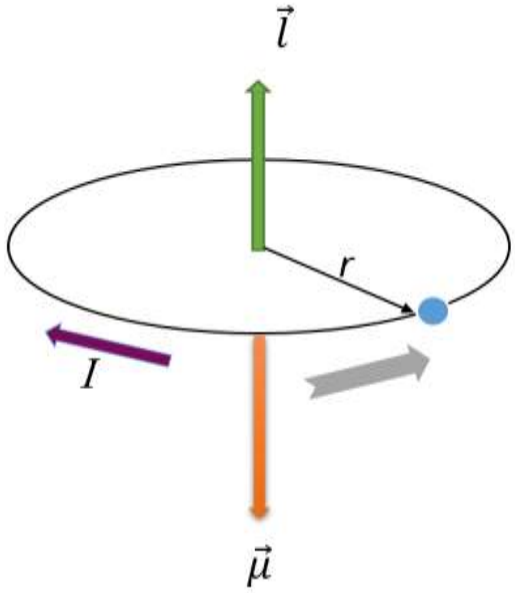


**Figure 2.1.** Orbital moment. The electron moves in circular orbit where its quantized angular momentum $\vec{l}$ and magnetic moment $\vec{\mu}$ are oppositely.

The basic unit of electron magnetism is called the Bohr magneton $\mu_B = 9.27 \times 10^{-21}\, erg/o_e$ which is the result of the orbital motion of one electron in the lowest orbit (Coey and Coey, 2010). Therefore orbital magnetic moment of an electron is given by

$$\mu_B = \frac{e\hbar}{2m_e} \qquad 2.5$$

In Bohr's quantum theory the z-component of orbital angular momentum $\vec{l}_z$ and spin angular momentum $\vec{s}_z$ is quantized in units of $\hbar$ where

$$\hbar = \frac{h}{2\pi} \qquad 2.6$$

And

$$\vec{l}_z = m_l \hbar\,, \qquad 2.7$$

where $m_l$ is a quantum number and $h$ is the Planck's constant.

This leads to

$$\mu_{lz} = -\frac{e\hbar}{2m_e} m_l = -\mu_B m_l \qquad 2.8$$

$$\mu_{sz} = -\frac{e\hbar}{m_e} m_s = -2\mu_B m_s \qquad 2.9$$

The orbital moments of all the electrons couple together to from the total orbital momentum expressed by

$$\vec{L} = \sum \vec{l}_i \qquad 2.10$$

The spins are also assumed to couple together to from the total spin momentums

$$\vec{s} = \sum \vec{s}_i \qquad 2.11$$

Finally through spin-orbit coupling $\vec{L}$ and $\vec{s}$ couple together

$$\vec{j} = \vec{s} + \vec{L} \qquad 2.12$$

This leads to the total magnetic moments of an atom in the direction of $\vec{j}$ to be expressed in the form

$$\vec{\mu}_J = -g\mu_B \vec{J}\,, \qquad 2.13$$

where $g$ is known as the landé g- factor which can easily be deduced to be (Coey and Coey, 2010)

$$g = 1 + \frac{J(J+1) + S(S+1) - L(L+1)}{2J(J+1)}, \qquad 2.14$$

when $g = 2$ the spin contribution arises and when $g = 1$ the orbital contribution arises. The mass of the nucleus is so large so the magnetic moments contribution can be neglected compared to the electronic magnetic moments.

## 2.3 Magnetization

The magnetic field strength is expressed by *H*. Here the magnetic flux density *B*, which is defined in terms of force on moving charge in the Lorentz force law (Good, 1999), expressed by

$$B = H + 4\pi M \tag{2.15}$$

Where, *M* is called magnetization which refer to the total magnetic moments $\mu$ in unit volume, given by

$$\vec{M} = \frac{1}{V}\sum_{i=1}^{N} \vec{\mu}_i \tag{2.16}$$

The magnetic properties of materials can be characterized by the magnitude of $M$ as function of $H$. The ratio between $M$ and $H$ is called the magnetic susceptibility $\chi$ of the sample and is taken by

$$\chi = \frac{M}{H} = \mu_0 \frac{M}{B_0} \tag{2.17}$$

where $B_0$ is a magnetic field, $\mu_0$ is magnetic permeability and defined by the equation

$$\mu = \frac{B}{H} \tag{2.18}$$

# Chapter Three

# Experimental details

# Chapter three
# Experimental details

This chapter contains the experimental techniques that were used in this work. Cobalt ferrite ($CoFe_2O_4$) nanoparticles produced by combustion, hydrothermal and glycol thermal methods. The X-rays diffraction technique was used to determine the crystal structure of the synthesized nanoparticles materials. The morphology was studied by high resolution transmission electron microscope. The magnetic properties were studied by vibrating sample magnetometer (VSM).

## 3.1 Synthesis techniques

Wet chemical synthesis methods such as combustion, hydrothermal and glycol thermal are widely used in producing nanomaterials. The main features of these methods are synthesizing uniform and relatively controlled size of nanoparticles. Metal chlorides or nitrates are commonly used as starting materials. In the present work the reagents were analytical grade and used as received from Sigma Aldrich chemical company without further purification. Cobalt nitrate ($CO(NO_2)_3.6H_2O$, 98%), ferric nitrate ($Fe(NO_3)_3.9H_2O_4$, 98%) were used as precursors. The urea ($CO(NH_2)_2$, 99%) was used as fuel only for combustion reaction.

### 3.1.1 Combustion method

Combustion synthesis is effective and low-cost method for producing nanomaterials. The basic principle of this method is forming a gel from metal salts and organic fuel such as urea, glycine or hydrazides. In this work, $CoFe_2O_4$ ferrite nanoparticles were prepared by adding the stoichiometric to 50 ml of deionized water and homogenized by a magnetic stirrer at 70 ℃. Ammonia hydroxide was added to the mixture until PH of 9 was reached. Then the mixture was then ignited to combust (Smoldering) with an evaporation of large amount of gases, giving a voluminous and foamy $CoFe_2O_4$ as a final product.

### 3.1.2 Hydrothermal method

Hydrothermal synthesis can be defined as a low temperature synthesis technique for producing nanoparticles. It depends on the solubility of metals chlorides or nitrates in hot water using closed-system. Advantages of the hydrothermal synthesis method include the ability to synthesize crystals of substances which are unstable near the melting point and also producing large crystals with high quality. However, disadvantages of this synthesis method

include high cost of equipment and the inability to monitor crystals in the process of their growth. In this work $CoFe_2O_4$ ferrite nanoparticles were prepared by dissolved Co $(NO_2)_3$ $.6H_2O$ and Fe $(NO_3)_3$ $.9H_2O_4$ in 50 ml deionized water to form a transparent solution, mixture was in round bottom flask. Then $NH_4OH$ solution was added to the above solution drop wise under magnetic stirring. The round bottom flask transferred to mantle heater at 100 ℃ for six hours. A condenser was used to condense the vapor back again into the round bottom flask. After the reaction was completed, the sample was dried using IR lamp. Figure 3.2 shows the experimental setup of hydrothermal method.

**Figure 3.1.** Experimental setup of hydrothermal method, Condensed Matter Physics Laboratory, Westville campus, University of KwaZulu-Natal, South Africa.

### 3.1.3 Glycol thermal method

The glycol thermal method is one of the methods used to synthesis nanoparticles. Used the ethylene glycol as synthesis medium and pressure reactor. In this action, $CoFe_2O_4$ nanoparticles were synthesized by adding stoichiometric metal chloride powders were dissolved in 400 mL of deionized water using a magnetic stirrer for 30 min. Drops of $NH_4OH$ solutions were added slowly to the mixture until a pH of about 9 was reached. The precipitate was reacted in 200 mL of ethylene glycol at 200℃ in a pressure reactor under continuous

stirring for 6 h at a pressure of about 100 Psi. After the reaction, the mixture was washed with deionized water over a fresh GF/F filter. The final product was dried overnight using a 200 W infrared lamp. Figure 3.2 shows a watlow stirred pressure reactor.

**Figure 3.2.** PARR 4843 stirred pressure reactor, Condensed Matter Physics Laboratory, Westville campus, University of KwaZulu-Natal, South Africa.

## 3.2 Structural techniques

### 3.2.1 X-rays diffractometer (XRD)

The X-rays diffraction XRD is considered to be essential method for crystallographic characterization for bulk, nano and thin film materials. It is one of most analytical techniques for determining the crystal structure of crystalline samples. The XRD technique identifies and quantifies various crystalline phases of powder and solid materials, all of which determine the physical properties of the sample. The lattice parameters, crystalline sizes, X-rays densities and microstrain can also be evaluated. Figure 3.3 shows schematic diagram of incident monochromatic beam of X-rays on crystalline sample.

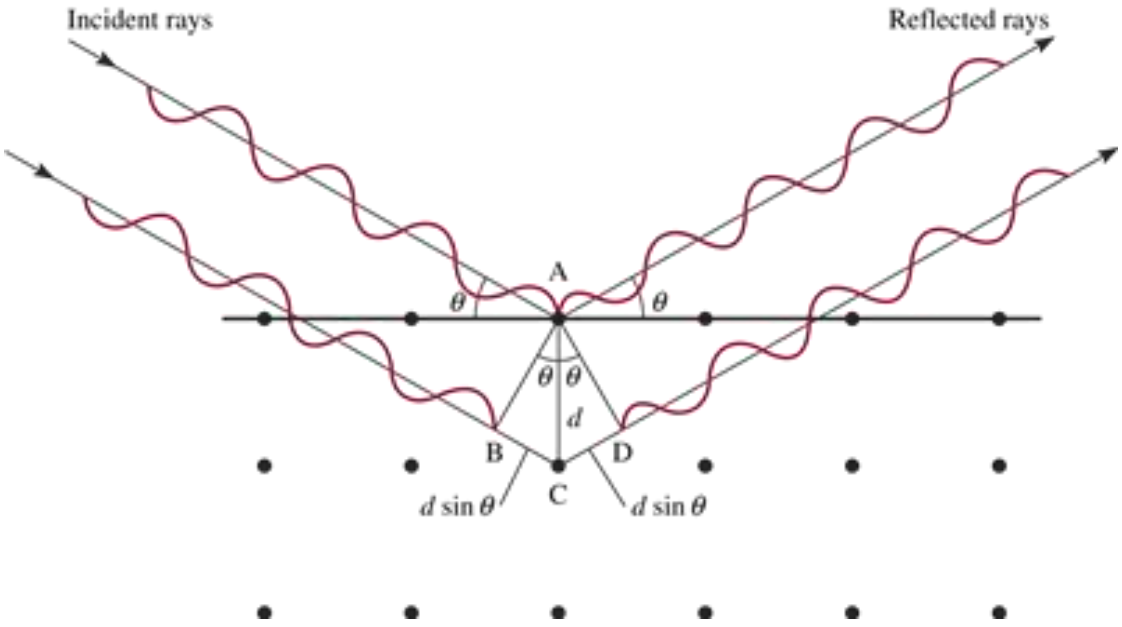


**Figure 3.3.** Schematic illustration the principle of X-rayss diffraction.

The constructive interference occurs when Bragg's law is satisfied

$$n\,\lambda\, =\, 2dsin\,\theta, \tag{3.1}$$

where $n$ is an integer number and $\theta$ is the angle between the incident beam and the scattering plane.

The relation between the inter-planar spacing $d$ and the lattice parameter $a$ of the cubic crystalline system calculated using Bragg's law (Nadir S.E. Osman, Thomas Moyo., 2015)

$$a = d(h^2 + k^2 + l^2)^{\frac{1}{2}}, \tag{3.2}$$

where $h$, $k$ and $l$ are Miller indices of particular plane (Nadir S.E. Osman, Thomas Moyo, 2015). In 1918, Scherrer observed the relationship between microstructure and the diffraction patterns. The equation describing the relationship between the crystallite size and the peak width, which is called the Scherer's formula (Liu et al., 2009)

$$D = k\lambda/\beta \cos\theta\,, \qquad 3.3$$

where *D* represents the size of the crystallites, λ is the wavelength of X-rayss, $\beta$ is the full width at half maximum,$\Theta$ is the Bragg angle of the (311) plane and *K* is the Scherer's constant. The Scherrer's constant (K) value of 0.9 is known as the crystal shape factor. This equation can be used to evaluate the crystallite size of nanomaterials. However, for more accurate values for crystallite sizes of a sample modified Scherrer's equation required (Monshi et al, .2012)

$$ln\beta = ln\frac{k\lambda}{l} + ln\frac{1}{cos\theta} \qquad 3.4$$

The X-rays densities can be calculated from the equation

$$\rho_{XRD} = 8M_0/N_A a^3, \qquad 3.5$$

where $M_0$ is the molecular weight and $N_A$ is the Avogadro's number. Figure 3.4 shows the X-ray diffractometer (Nadir S.E. Osman and Thomas Moyo, 2015).

The microstrain ($\varepsilon$) values were calculated using the equation

$$\varepsilon = \beta/4\tan\theta, \qquad 3.6$$

where $\varepsilon$ is the microstrain (Nadir S.E. Osman and Thomas Moyo, 2015). Figure 3.4 shows the Phillips XRD diffractometer Model: PANalytical, EMPYREAN was used for structure determination in this work. The instrument uses a CoKα radiation source ($\lambda$=1.7903 Å).

**Figure 3.4.** Empyrean PANalytical X-ray diffractometer cabinet, Geology Westville campus, University of KwaZulu-Natal, South Africa.

### 3.2.2 High resolution transmission electron microscope (HRTEM)

High resolution transmission electron microscopy (HRTEM) is basically create well defined interference images for nanoparticles by using transmitted and scattered beams. The principle of HRTM depends on transmitting a focuses, high beam through an ultra-thin sample to provide important information about morphology, crystalline quality, particle sizes, and distribution. The image of nanoparticles is formed when the electron beam reflects mainly from the surface of the sample (Erni et al, 2009). Figure 3.5 shows high resolution transmission electron microscope (HRTEM).

**Figure 3.5.** Joel-JEM-2100 high resolution transmission electron microscope, Westville campus, University of KwaZulu-Natal, South Africa.

### 3.2.3 Lake Shore model 735 vibrating sample magnetometer (VSM)

Vibrating sample magnetometer (VSM) is used to measure the magnetization of samples. The principle of VSM is based on faraday's law (Pradeep et al., 2008)

$$\frac{d\phi}{dt} = -E, \qquad 3.7$$

where □ is the magnetic flux and *E* is induced voltage in the pick-up coils. Magnetic amounts of a sample play essential role in determining its magnetic behavior. The magnetization of the sample is proportional to the induced voltage. The change in flux is caused by vibrating the

sample at fixed frequency. Figure 3.6 shows lake shore model 735 vibrating sample magnetometer (VSM).

**Figure 3.6.** LakeShore model 735 vibrating sample magnetometer (VSM), Condensed Matter, University of KwaZulu-Natal, South Africa.

# Chapter Four

# Results and discussion

# Chapter four

# Results and discussion

This chapter contains the analysis of X-rays diffraction, vibrating sample magnetometer results and high resolution transmission electronic microcopy of the cobalt ferrite nanoparticles samples prepared by combustion, hydrothermal and glycol thermal methods.

## 4.1 X-rays diffraction study

Table 4.1 shows the calculated vales of lattice parameters ($a$), crystallite sizes ($D$) and X-rays densities ($\rho_{XRD}$). The lattice parameter ($a$) was calculated using Bragg's law as in equation 2.1. The lattice parameters were computed from the highest intensity peak and found to be 8.339Å, 8.352 Å and 8.383 Å for combustion, hydrothermal and glycol thermal methods are respectively. The X-rays patterns of all samples were fitted by Full Proof software program. The obtained lattice parameters were 8.371 Å, 8.345 Å and 8.365 Å, and for combustion, hydrothermal and glycol thermal and methods. Slightly difference was observed between the lattice parameters that calculated from highest intensity peaks and the ones obtained from fitting process. This could be due to the background on the X-rays patterns which may affect the fitting processes. The calculated lattice parameter are close to the reported theoretical value of $a$ = 8.392 Å (F.amrouche et al., 2018).

The structure of the samples were studied by X-rays diffraction (XRD). Figure 4.1 shows the XRD patterns of $CoFe_2O_4$ samples prepared by combustion, hydrothermal and glycol thermal methods. The obtained X-rays diffraction peaks are well defined and indexed as (111), (220), (311), (222), (400), (422), (511) and (440), which are characteristics of single phase cubic spinel structure with space group f*d*-3m (A. Manikandan et al, 2013). Since no additional phase were observed, hence, the obtained results are in agreement with JCPDS standard card no.01-077-0426 (Houshiar et al., 2014). This were also confirmed by $CoFe_2O_4$ nanoparticles the best fitting obtained using Full proof software program for x-rays pattern of the samples.

The crystallite sizes were calculated using modified Scherer's formula as mentioned in the equation 3.4. The highest value of the crystallite sizes of 23.296 nm obtained for the sample prepared by combustion method. Whilst, the crystallite sizes for samples prepared by hydrothermal and glycol thermal methods were found to be 9.168 nm and 7.910 nm,

respectivley. The crystallite sizes increases as synthesis temperature increases due to centering of nanoparticles (Houshiar et al., 2014).

X-rays diffraction densities ($\rho_{XRD}$) were calculated using equation 3.5. The highest density was noticed for the sample prepared by combustion method with the value of 5.379 g/cm$^3$ whereas, the sample prepared by glycol thermal method possessed the lowest X-rays density with the value of 5.295g/ cm$^3$. The microstrain ($\varepsilon$) values were calculated using the equation 3.6. The obtained values of microstrain were 0.00501 ± 0.00010, 0.01525 ± 0.00011 and 0.01243 ± 0.00016 for combustion, hydrothermal and glycol thermal methods, respectively. The variation in microstrain values is associated with the change in synthesis temperature. The sample prepared by the combustion method is expected to have less value of microstrain. This is because the reaction temperature of combustion method are higher compared to glycol thermal and hydrothermal methods. Therefore, atoms might have enough kinetic energy so they placed properly inside the lattice cell.

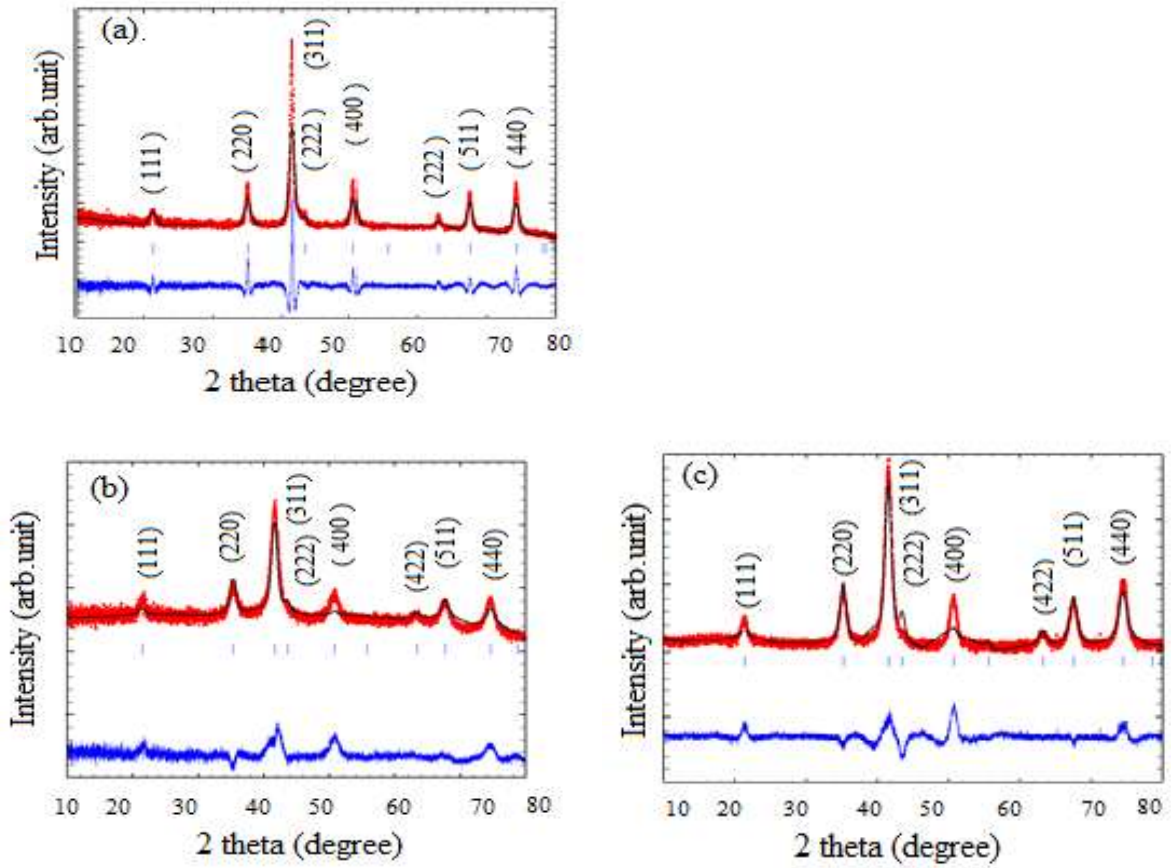


**Figure 4.1.** Refinement of X-rays diffraction patterns of $CoFe_2O_4$ prepared by (a) combustion, (b) hydrothermal and (c) glycol thermal methods.

**Table 4.1.** Lattice parameters ($\boldsymbol{a}$), crystallite sizes ($\boldsymbol{D}$), X-rays densities ($\boldsymbol{\rho_{XRD}}$) and microstrains ($\boldsymbol{\varepsilon}$) of $CoFe_2O_4$ sample of prepared by combustion, hydrothermal and glycol thermal methods.

| Sample | $D_{XRD}$ (nm) ± 0.093 | $a$ (Å) ± 0.007 | $\rho_{XRD}$ (g/cm$^3$) | $\varepsilon$ ±0.00005 |
|---|---|---|---|---|
| Combustion method | 23.296 | 8.339 | 5.379 | 0.00501 |
| Hydrothermal method | 7.910 | 8.352 | 5.353 | 0.01525 |
| Glycol thermal method | 9.168 | 8.383 | 5.295 | 0.01243 |

## 4.2 High resolution transmission electronic microcopy study

The microstructure of the samples were studied by high resolution transmission electronic microcopy (HRTEM). Figure 4.2 represents HRTEM images of $CoFe_2O_4$ samples prepared by combustion, hydrothermal and glycol thermal methods. The values of the particle sizes estimated from the images indicated that the synthesized samples are in nanoscales. Furthermore, the nanoparticle sizes are less than 100 nm. From the images, the bright stripes called lattice fringes resultant from interface when the beam of X-rays hit the samples. Since lattice fringes appeared clearly as seen from HRTEM images in figure 4.2, hence the synthesized samples are well crystalline.

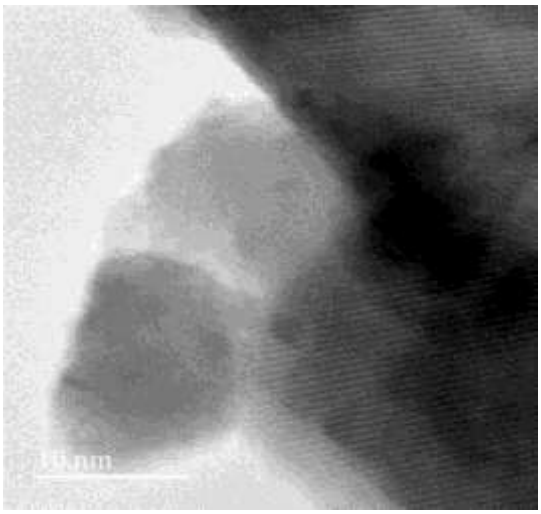

( a )

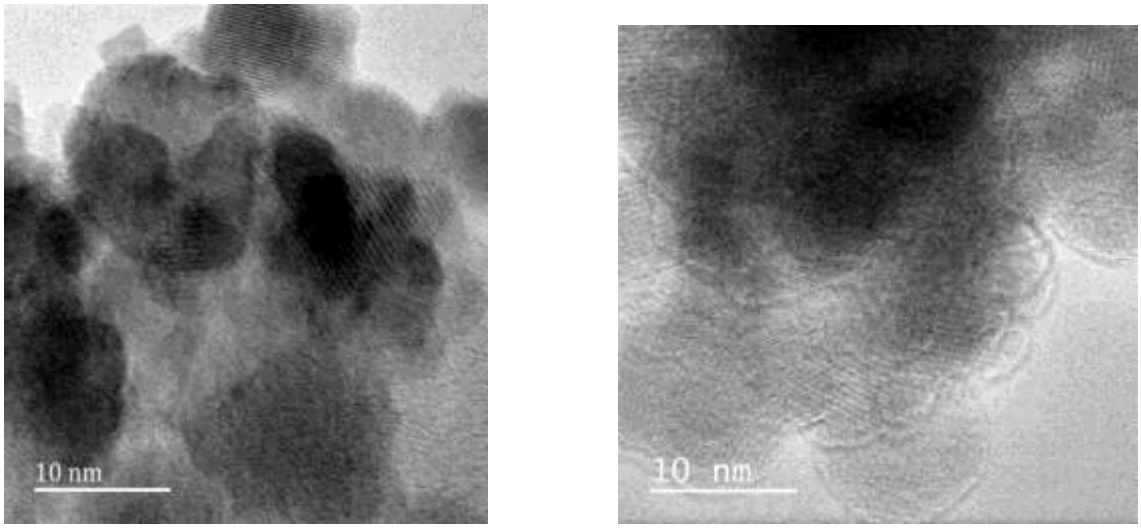


(b) (c)

**Figure 4.2.** HRTEM images of the $CoFe_2O_4$ nanocrystals synthesized by (a) combustion, (b) hydrothermal and (c) glycol thermal methods.

## 4.3 Vibrating sample magnetometer measurements

The magnetic properties of $CoFe_2O_4$ samples were studied at room temperature by vibrating sample magnetometer (VSM). Figure 4.3 showed the hysteresis loops of $CoFe_2O_4$ samples prepared by combustion, hydrothermal and glycol thermal methods. The maximum magnetization value ($M_s$), coercivity ($H_c$), remnant magnetization ($M_R$), magnetic moment ($n_B$) and squareness ratio ($M_R/M_s$) are presented in table 4.2. The maximum magnetization value of 56.06 ± 0.13 emu/g and highest value of coercivity of 1277.6 ± 0.001 Oe obtained for the sample prepared by combustion method. This expected to be due to the highest value of crystallite sizes of 23.296 ± 0.093 nm obtained for this particular sample. The results show that the coercivity and maximum magnetization are significantly depend on the crystallite sizes. The obtained trend between coercivity and magnetization are in agreement with the reported one by Yang et al (Yang et al., 2006). The remnant magnetization for glycol thermal, combustion and hydrothermal methods are 2.449 emu/g, 21.25 emu/g and 3.948 emu/g, respectively.

The magnetic moments ( $n_B$) were calculated from $M_s$ (emu/g) using the formula (Singhal, 2010).

$$n_B = M_0 \times M_s/5585, \qquad 4.1$$

where $M_s$ maximum magnetization. The squareness of the hysteresis loop is associated to the values of $M_R/M_s$. Moreover, it indicates whereas the sample is soft or hard magnetic material. This can be a useful guide in practical applications of materials (Nadir S.E. Osman, Thomas Moyo., 2015).

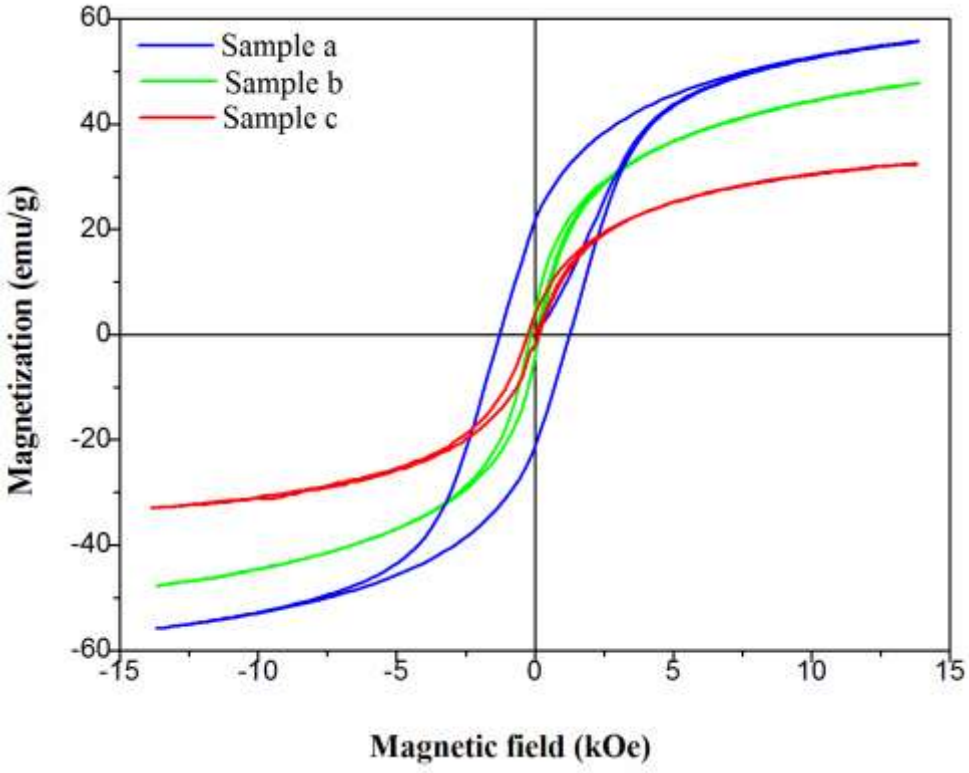


**Figure 4.3.** Room temperature hysteresis loops of $CoFe_2O_4$ sample prepared by (a) combustion, (b) hydrothermal and (c) glycol thermal methods.

**Table 4.2.** Coercivity ($H_c$), remnant magnetization ($M_R$), maximum magnetization ($M_s$), magnetic moment ($n_B$) and squareness ratio ($M_R/M_s$) of $CoFe_2O_4$ prepared by hydrothermal, combustion and glycol thermal methods.

| Sample | $\boldsymbol{H_c}$(Oe) ± 0.001 | $M_R$(emu/g) ± 0.0002 | $\boldsymbol{M_s}$(emu/g) ± 0.13 | $\boldsymbol{M_R/M_s}$ | $\boldsymbol{n_B(\mu_B)}$ |
|---|---|---|---|---|---|
| Combustion method | 1277.6 | 21.25 | 56.06 | 0.379 | 0.0031 |
| Hydrothermal method | 175.12 | 3.948 | 47.74 | 0.082 | 0.0097 |
| Glycol thermal method | 199.95 | 2.449 | 32.71 | 0.074 | 0.0006 |

## 4.4 Conclusion

Structure and magnetic properties of $CoFe_2O_4$ nanoparticles synthesized by combustion, glycol thermal and hydrothermal methods were investigated. The formation of cubic spinal phase with space group fd-3m for $CoFe_2O_4$ nanoparticles was confirmed using X-rays technique. The average crystallite sizes were estimated using modified Scherrer's formula to be 23.296 nm, 7.910 nm and 9.203 nm for combustion, hydrothermal, and glycol thermal methods, respectively. Glycol thermal and hydrothermal methods were noticed to produce highly strained $CoFe_2O_4$ nanoparticles compared to combustion method. Magnetic properties of nanocrystalline $CoFe_2O_4$ samples were investigated by using vibrating sample magnetometer. The data showed that the maximum magnetization value of 56.06 emu/g and highest value of corecivity of 1277.6 Oe obtained for the sample prepared by combustion method. The results confirm that various synthesis methods of nanoparticle can lead to different particle sizes and then significantly affect the magnetic properties.

## 4.5 Recommendations

In the light of the findings of this study, some recommendation can be suggested which may lead to get best results for similar study

- Saturation magnetization can be obtained by fitting initial magnetization carves.
- Average particle sizes can be calculated from the TEM scanning electronic microscope images.
- Additional information about structure such as atoms position and molecule bonding can be obtained from Full Proof results.

## 4.6 Future work

Simple and relatively cost-effective methods were used to prepare cobalt ferrite nanoparticle. For any future study the following features can be considered

- Preparing cobalt ferrite nanoparticles by using more synthesis methods such as micro-emulsion, microwave, sol-gel and co-precipitation.
- Study the electrical and optical properties of synthesized cobalt ferrite nanoparticles.
- Further Structural characterizations can be achieved by techniques such as Fourier transform infrared (FTIR), high resolution scanning electronic microscopy (HRSEM), Brunauer-Emmett-Teller (BET).
- Since magnetization behavior of a material is significantly affected by temperature, the *M-H* loops as a function of measuring temperatures is highly recommended as a Future work.

## 4.7 References


Coey, J. M. D. & Coey, J. M. D. 2010. Magnetism and Magnetic Materials, Cambridge University Press.

Dekker, Adrianus J. 1981, Ferromagnetism, Antiferromagnetism, and Ferrimagnetism, Solid State Physics, 464-497.

Erni, R., RosselL, M.D., Kisielowski, C. and Dahmen, U., 2009. Atomic-resolution imaging with a sub-50-pm electron probe. Physical review letterss, 102(9), p.096101.

F.Amrouche-Boumezoued1, N. Bendjaballah-Lalaoui, S.Rennane, N. Fodil Cherif, A. Djadoun and Y. Hammiche-Bella., 2018. Synthesis and Caracterisation of Spinel CoFe2O4: Application for Methylene Blue Photocatalytic Degradation, Bridging science and technology.

Franco, A., Celma, D., E.Oliveira Lima, E., Novak, M. A. & Wells, P. R. 2007. Synthesis of nanoparticles of $Co_xFe_{(3-x)}O_4$ by combustion reaction method. Journal of Magnetism and Magnetic Materials, 308, 198-202.

Good, R. H. 1999. Classical Electromagnetism, Saunders College Pub.

Horikoshi, S. & Serpone, N. 2013. Introduction to Nanoparticles. Microwaves in Nanoparticle Synthesis. Wiley-VCH Verlag GmbH & Co. KGaA.

Houshiar, M., Zebhi, F., Razi, Z. J., Alidoust, A. & Askari, Z. 2014. Synthesis of cobalt ferrite ($CoFe_2O_4$) nanoparticles using combustion, coprecipitation, and precipitation methods: A comparison study of size, structural, and magnetic properties. Journal of Magnetism and Magnetic Materials, 371, 43-48.

Khandekar, M. S., Kambale, R. C., Patil, J. Y., Kolekar, Y. D. & Suryavanshi, S. S. 2011. Effect of calcination temperature on the structural and electrical properties of cobalt ferrite synthesized by combustion method. Journal of Alloys and Compounds, 509, 1861-1865.

Krasnovyd, S. V., Konchits, A. A., Shanina, B. D., Valakh, M. Y., Yanchuk, I. B., Yukhymchuk, V. O., Yefanov, A. V. & Skoryk, M. A. 2015. Local structure and paramagnetic properties of the nanostructured carbonaceous material shungite. Nanoscale Research Letters, 10, 78.

Liu, Y., Zhang, Y., Feng, J. D., LI, C. F., SHI, J. & Xiong, R. 2009. Dependence of magnetic properties on crystallite size of $CoFe_2O_4$ nanoparticles synthesised by auto-combustion method. Journal of Experimental Nanoscience, 4, 159-168.

Mathew, D. S. & Juang, R.-S. 2007. An overview of the structure and magnetism of spinel ferrite nanoparticles and their synthesis in microemulsions. Chemical Engineering Journal, 129, 51-65.

Monshi, A., Foroughi, M.R. and Monshi, M.R., 2012. Modified Scherrer equation to estimate more accurately nano-crystallite size using XRD. World Journal of Nano Science and Engineering, 2(3), pp.154-160.

Nadir S.E. Osman, Thomas Moyo., (2015), Structural and magnetic properties of $CoFe_2O_4$ nanoferrite simultaneously and symmetrically substituted by Mg, Sr and Mn. Materials Chemistry and Physics, pp.1–7.

Nadir, O.S., Thapliyal, N., Alwan, W.S., Karpoormath, R. and Moyo, T., 2015. Synthesis and characterization of $Ba_{0.5}Co_{0.5}Fe_2O_4$ nanoparticle ferrites: Application as electrochemical sensor for ciprofloxacin. Journal of Materials Science: Materials in Electronics, 26(7), pp.5097-5105.

Nagamiya, Takeo, 1951, Theory of Antiferromagnetism and Antiferromagnetic Resonance Absorption, Progress of Theoretical Physics, 6, 342-349.

Peng, J., Hojamberdiev, M., Xu, Y., Cao, B., Wang, J. & WU, H. 2011. Hydrothermal synthesis and magnetic properties of gadolinium-doped $CoFe_2O_4$ nanoparticles. Journal of Magnetism and Magnetic Materials, 323, 133-137.

Pradeep, A., Priyadharsini, P. & Chandrasekaran, G. 2008. Sol–gel route of synthesis of nanoparticles of $MgFe_2O_4$ and XRD, FTIR and VSM study. Journal of Magnetism and Magnetic Materials, 320, 2774-2779.

Qu, Y., Yang, H., Yang, N., Fan, Y., Zhu, H. and Zou, G., 2006. The effect of reaction temperature on the particle size, structure and magnetic properties of coprecipitated $CoFe_2O_4$ nanoparticles. Materials Letters, 60, 3548-3552.

Rohollah Safi, Ali Ghasemi, Reza Shoja-Razavi, Ebrahimghasemi, Tahmineh Sodaee.2016. Rietveld structure refinement, cations distribution and magnetic features of $CoFe_2O_4$ nanoparticles synthesized by co-precipitation, hydrothermal, and combustion methods. Ceramics International, 42, 6375-6382.

Singhal, S. 2010. Effect of Zn Substitution on the Magnetic Properties of Cobalt Ferrite Nano Particles Prepared Via Sol-Gel Route. Electromangtic analysis and applications, 2, 376-381.

Simon, M. D. & Geim, A. K. 2000. Diamagnetic levitation: Flying frogs and floating magnets (invited). Journal of Applied Physics, 87, 6200-6204.

Sawatzky, G.A., Van Der Woude, F. and Morrish, A.H., 1968. Cation distributions in octahedral and tetrahedral sites of the ferrimagnetic spinel $CoFe_2O_4$. Journal of Applied Physics, 39, 1204-1205.

William Fuller Brown Jr, 1940, Ferromagnetic Domains and the Magnetization Curve, Journal of Applied Physics, 11, 160-172.